ACS OMEGA

Open Access

http://pubs.acs.org/journal/acsodf

Article

Enhanced and Sustained Transdermal Delivery of Oxypurinol Using Thermosensitive Gel Combined with Polymeric Solid Microneedles

Siti Nur Fatimah S. Mohamad, Stephanie Stephanie, Zulfiayu Sapiun, Frederika Tangdilintin, Sulistiawati Sulistiawati, Achmad Himawan, Yusnita Rifai, Habibie Habibie, Aliyah Aliyah, Muhammad Aswad, and Andi Dian Permana*

Cite This: *ACS Omega* 2025, 10, 3500−3510

Read Online

ACCESS | Metrics & More | Article Recommendations

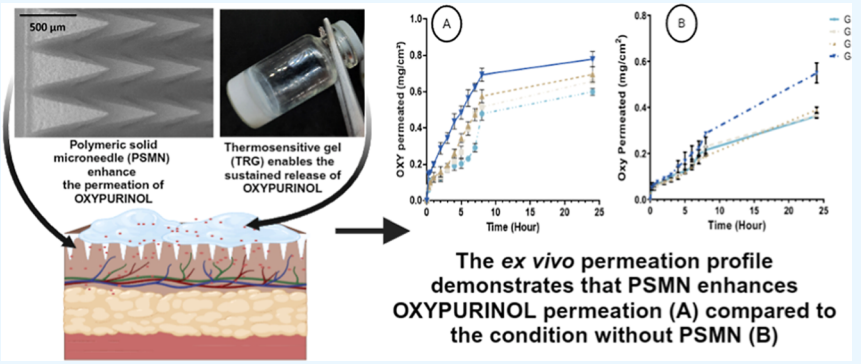

ABSTRACT: Gout is a pathological condition caused by monosodium urate crystal deposition in tissues. Allopurinol, the first-line therapy, inhibits xanthine oxidase but may be ineffective due to reduced conversion to oxypurinol (OXY). Current delivery routes for OXY, including oral and intravenous routes, have drawbacks such as poor solubility and patient discomfort. This study developed a delivery system integrating thermosensitive gel (TRG) containing OXY with polymeric solid microneedles (PSMNs). Molecular docking demonstrated high-affinity binding interactions between OXY and Pluronic (−2.5). The TRG, formulated with Pluronic F127 and F68, was assessed for gelation temperature, pH, spreadability, and bioadhesive strength. PSMN, made from poly(vinyl alcohol) and polyvinylpyrrolidone K-30 with citric acid, was evaluated for mechanical strength and skin penetration. In vitro hemolysis activity, drug release, and ex vivo permeation studies were conducted. Molecular docking results showed stable binding with an affinity of −2.5 between the ligands of OXY and Pluronic. The TRG formulation exhibited promising characteristics for transdermal drug delivery. PSMN demonstrated good mechanical strength and was able to penetrate up to 504 μm. Hemolysis testing showed that PSMN and TSG were safe with a hemolysis ratio of less than 5%. In vitro drug release studies showed a high OXY release of 2.24 ± 0.26 mg with the highest concentration of Pluronic F68, displaying a sustained release profile. Ex vivo permeation studies showed a significant difference ($p < 0.05$) between OXY permeation without and with PSMN combination. PSMN increased OXY permeation by 79−81% compared to permeation without PSMN. This study successfully developed a TRG formulation combined with PSMN to enhance transdermal delivery of OXY. These results suggest a promising new route for OXY delivery, potentially offering a more efficient and user-friendly treatment for chronic gout. Further in vivo studies are needed to evaluate the efficacy, pharmacokinetics, pharmacodynamics, drug interactions, and toxicity for further clinical applications.

1. INTRODUCTION

Gout is a pathological condition resulting from monosodium urate crystal deposits in tissues. This condition is typically triggered by high uric acid crystals in the blood (hyperuricemia).[1] Excess uric acid crystals deposit in specific body areas (usually the joints) and can cause gout.[2] Prolonged gout can lead to bone erosion, cartilage damage, the formation of tophi, and comorbid diseases affecting the cardiovascular, renal, metabolic, neurological, and ophthalmological systems.[1,3] According to the global burden of gout data from 2019, the number of gout cases worldwide reached approximately 53.87 million. Over the past 30 years, the prevalence of gout has increased in nearly all regions of the world. The age-standardized

Received: August 20, 2024
Revised: December 8, 2024
Accepted: December 13, 2024
Published: December 20, 2024

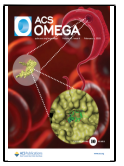

prevalence, incidence, and disability-adjusted life years (DALYs) also showed an acceleration during the 1990−2019 period, with an annual growth rate of approximately 0.77% to 0.94%, particularly among men.[4]

The first-line therapy for chronic gout is allopurinol, which acts as an inhibitor of xanthine oxidase (XO) enzyme. Allopurinol can reduce uric acid levels by inhibiting the XO enzyme involved in the purine catabolism pathway, where hypoxanthine is converted into xanthine and then into uric acid.[5,6] However, there have been studies suggesting that allopurinol may be ineffective in reducing uric acid levels due to a possible decrease in the conversion of allopurinol to oxypurinol (OXY), resulting in the continued formation of uric acid.[7] Therefore, alternative XO inhibitors, such as OXY, should be considered. OXY is an XO inhibitor with a longer half-life of approximately 13−18 h compared to allopurinol, which has a shorter half-life of about 1−1.6 h. Consequently, allopurinol requires more frequent dosing than OXY.[8,9]

Various drug delivery routes have been developed, including oral, sublingual, rectal, parenteral, transdermal, and others.[10] Currently, gout treatment is generally administered through oral and intravenous (IV) routes. OXY can be formulated for delivery through these two routes; however, there are several drawbacks to both oral and IV routes, such as the poor solubility of OXY due to its water insolubility. Additionally, oral administered drugs undergo first-pass metabolism and gastrointestinal enzyme activity, hindering drug absorption.[8,11] The IV route requires the use of needles, which can cause pain, necessitate medical assistance, generate medical waste, and increase the risk of infection due to improper injection. It can lead to patient noncompliance or even refusal of treatment.[12,13] Chronic gout treatment often requires long-term management; therefore, patient comfort is crucial. Transdermal drug delivery systems (TDDSs) allow for self-administration and convenience, with less frequent dosing compared to IV or oral therapies.[14,15]

TDDS can serve as a method of addressing these problems. TDDS has several benefits compared to oral drug delivery, including the potential to bypass first-pass metabolism, improve bioavailability, and minimize gastrointestinal side effects. Thermosensitive gel (TRG) formulations show the potential to decrease the frequency of drug delivery. TRG undergoes sol−gel transition in response to variations in temperature. The change in temperature induces a transformation from a sol state to a gel state, wherein polymers transition from a scattered micelle arrangement to a compact three-dimensional network structure.[16,17] Pluronic F127 (PL-127) and Pluronic F68 (PL-68) are often employed polymers in TRG formulations.[18,19] PL-127 and PL-68 are triblock copolymers consisting of a hydrophobic poly(propylene oxide) (PPO) core surrounded by hydrophilic poly(ethylene oxide) (PEO) on both sides.[20] The TRG micelle technology encapsulates OXY, enabling sustained release behavior. The sustained release behavior can decrease the frequency of medication doses and improve patient comfort and adherence throughout gout treatment. PL-127 and PL-68 exhibit distinct physicochemical characteristics, including variations in molecular weight and PPO/PEO ratios, which can influence micelle formation and gel viscosity. The objective of this study is to vary the composition of PL-68 in order to obtain the most favorable gel properties. In order to obtain more accurate data regarding the specific impacts of PL-68 on the properties and durability of the gel, one can vary the concentration of PL-68 while maintaining a constant concentration of PL-127. An obstacle in the transportation of OXY into the bloodstream through TRG is the existence of the stratum corneum (SC), which serves as the primary defense mechanism safeguarding the body against the external environment.[21] Consequently, applying OXY will encounter obstacles when passing through the SC. In order to improve the administration of OXY, a polymeric solid microneedle (PSMN) is used in combination with TRG as a pretreatment.

A PSMN is a microneedle made from polymers such as poly(vinyl alcohol) (PVA), polyvinylpyrrolidone (PVP), and cross-linkers. PSMN can penetrate the SC and create pores in the skin with microsized needles (25−1000 μm).[22−25] PSMN administration does not induce pain as the needles do not contact nerve endings, preventing patients from experiencing pain.[13,26] Furthermore, the PSMN formulation materials include biocompatibility and biodegradability and are user-friendly, hence establishing PSMN as a favored option.[27] Prior research has demonstrated that using solid microneedles in conjunction with TRG administration can enhance the penetration of drugs into the skin.[28,29]

Therefore, this study presents an innovative drug delivery system for the OXY formulation to treat hyperuricemia. For the first time, OXY is formulated in a TRG system combined with PSMN as a pretreatment. The characteristics of the TRG (GTR-OXY) are evaluated in terms of drug content, gelation temperature, pH, spreadability, bioadhesive strength, and in vitro drug release. At the same time, the PSMN is assessed for morphology, mechanical strength, and insertion capability. Finally, to test the permeation of this innovative GTR-OXY approach, ex vivo permeation studies are conducted, comparing results with and without PSMN.

2. MATERIALS AND METHODS

2.1. Materials. OXY of analytical grade was obtained from Tokyo Chemical Industry (Tokyo, Japan). PL-127 and PL-68 were generously provided by BASF Indonesia, Jakarta. PVP K-30 was obtained from Fadjar Kimia in Bogor, Indonesia, while PVA was acquired from Sigma-Aldrich Pte Ltd. in Singapore. All supplementary materials used were of high-quality analytical grade.

2.2. Molecular Docking. Molecular docking is a computer method used to forecast the binding strength of ligands to receptors. This study simulated the affinity between OXY as the ligand and Pluronic as the receptor. OXY affinity was compared with PL-127 and PEG as a comparator. The 3D structures of OXY and PL-127 were obtained from the PubChem database (OXY CID: 135398752 and PL-127 CID: 10154203). Analysis was performed using UCSF Chimera software version 1.17 for visualization, analysis, and molecular structure modeling. In this analysis, the ligands and receptors were prepared using the "Dock Prep" feature in Chimera to achieve geometric optimization and energy minimization. Subsequently, AutoDock Vina software was used to optimize the placement of ligands in the receptor binding site by forming a grid box encompassing the entire molecule.[30−33] The grid box dimensions are detailed in Table 1. The results of the binding affinity and intermolecular hydrogen bonds obtained were recorded.

2.3. Design of the Formulation. Table 2 presents detailed information regarding the composition and properties of the TRG formulation of X-ray ionization (TRG-OXY). TRG-OXY was made by a modified cold technique, in which PL-127 and PL-68 were gradually added to cold distilled water (4 °C). A

https://doi.org/10.1021/acsomega.4c07716
ACS Omega 2025, 10, 3500−3510

Table 1. Grid Box Size in Molecular Docking Analysis

reseptor—ligand	grid center (x; y; z)	grid size (x; y; z)
pluronic F127—OXY	−0.33; 0.0175; 0.121	26.72; 24; 15.99; 12.74
polyethylene glycol—OXY	−0.132; 0; −0.3	13.42; 7.89; 7.47

Table 2. Composition of TRG-OXY Formulations

composition	% composition			
	G1	G2	G3	G4
pluronic F127 (PL-127)	19	19	19	19
pluronic F68 (PL-68)	0	6.7	7.7	8.7
oxypurinol (OXY)	1	1	1	1
distilled water	Ad 100			

magnetic stirrer continually agitated the mixture until a homogeneous poloxamer solution was obtained. The solution was chilled until it became clear. Subsequently, the OXY compound was added to the poloxamer solution and thoroughly mixed until a homogeneous mixture was achieved.[18]

2.4. Drug Content. An aliquot of 0.1 mL of TRG-OXY (equivalent to 10 mg of OXY) was dissolved using NaOH 0.1N, sonicated for 10 min, and centrifuged for 10 min. The supernatant was determined using a UV−vis spectrophotometer (Dynamica, HALI XB-10, UK). Drug content was estimated using the calibration curve equation from standard solutions in NaOH 0.1N (2.5−80 μg/mL).[29]

2.5. Evaluation of Thermosensitive Gel Properties. *2.5.1. Temperature$_{sol-gel}$ Test.* The gelation temperature was assessed by using a modified vial technique. Each vial containing 2 mL of the gel formulation was initially stored at 4 °C. These vials were then submerged in water at 20 °C and subjected to a gradual heating process, increasing the temperature by 1 °C increments up to 65 °C. At each temperature increment, the vial was tilted to a 90° angle to visually inspect the gel. The gelation temperature was determined as the temperature at which the formulation stopped flowing and transformed into a solid gel state.[18] The experiment was conducted with replication.

2.5.2. pH Measurement. The pH of the gel formulation was determined by inserting the electrode at room temperature using a digital pH meter (Horiba Scientific, Kyoto, Japan), and the measurements were recorded in triplicate.[29]

2.5.3. Spreadability Test. 5 g of gel sample was placed between two glass plates. A 500 g weight was applied to the top plate for 5 min to exert pressure. The spreadability of the gel was then measured and recorded using a caliper (Tricle brand, Shanghai China).[34] The test was carried out in triplicate.

2.5.4. Bioadhesive Strength Test. The bioadhesive strength test was conducted using rat skin and rinsed with PBS at pH 7.4 before use. Wistar rat skin was employed as the membrane between the upper and lower vials. A gram of gel was applied onto the membrane of the lower vial, and the two vials were then aligned to ensure contact between the membrane surfaces, maintaining this position for 2 min. Additional weights were incrementally added to the opposite side of the balance until the separation of the vials occurred.[19] The minimum weight necessary to achieve vial separation was quantified to assess the mucoadhesive strength, utilizing eq 1 as described below

$$\text{muchoadhesion streght (dyne} \times \text{cm}^2) = \frac{m \times g}{A} \quad (1)$$

where m is the mass needed to separate the two vials (g), g represents the gravitational constant (980 cm/s^2), and A denotes the area of the exposed membrane (cm^2).

2.6. Formulation and Evaluation of the Polymeric Solid Microneedle. *2.6.1. Formulation of the Polymeric Solid Microneedle.* PSMNs were fabricated using PVA and PVP polymers, with citric acid as a cross-linker. PVA 5% and PVP K-30 15% (w/w) solution was prepared by dissolving the polymers in water. The solution was then placed in an oven at 80 °C for 1 h. The mixture of PVA and PVP solution was homogenized, and cross-linker citric acid was added and mixed thoroughly. The mixture was transferred into molds and centrifuged at 3100 rpm for a total duration of 2 × 30 min. After centrifugation, the molds were dried at 37 °C for 48 h. The resulting microneedles were then separated from the molds and placed in an oven at 80 °C for 1 h.[35,36] The PSMNs were stored under controlled conditions to maintain their integrity until further testing and characterization.

2.6.2. Morphology of PSMN. Subsequently, the PSMNs were subsequent for their morphological characteristics, which were examined in a light microscope using an Optilab camera (Olympus CS33, Japan) at 4× magnification. Additionally, the morphology of the PSMN was analyzed using a scanning electron microscope (Hitachi TM3030, Tokyo, Japan) to observe the needle shape and structure in detail.[32,37]

2.6.3. Mechanical Strength Test. The mechanical strength of the microneedle was determined through a mechanical strength test. This test used parafilm as a skin simulation. The parafilm was carefully folded into eight layers, each about 1 mm thick, and securely attached to a plexiglass sheet to provide a stable support. The PSMN was positioned atop the parafilm, and a load of 32 N was applied to the PSMN for 30 s. The height of PMNS before and after testing was measured using a light microscope.[38] The indicator of mechanical strength was calculated by the percentage of needle height reduction (HR) using eq 2.

$$\text{Height reduction percentage (\% HR)} = \frac{H_a - H_b}{H_a} \times 100\% \quad (2)$$

where H_a represents the needle height before testing, while H_b refers to the needle height after testing.

2.6.4. Insertion Test. The study aimed to assess the skin penetration potential of the PSMN through an insertion test. PSMN was positioned on parafilm, and a force of 32 N was applied to its surface for 30 s. Subsequently, the measurement of perforations in each parafilm was conducted.[38] The insertion ability of the PSMN was calculated using eq 3

$$\text{insertion ability percentage (\%)} = \frac{\text{number of holes in n layer}}{\text{total number of holes}} \times 100\% \quad (3)$$

2.7. In Vitro Hemolysis Test. Blood for the hemolysis test was obtained from healthy Wistar rats. The collected blood was separated into erythrocytes and other blood components using a centrifuge at 2000 rpm for 20 min. The erythrocyte pellet was isolated from the supernatant and washed three times with a PBS solution at pH 7.4. The erythrocytes were subsequently resuspended in PBS to reach a final concentration of 10% v/v. Test solutions, including PSMN and TRG-OXY, were diluted in PBS at pH 7.4 to reach concentrations of 5, 50, and 500 μg/mL in 900 μL of each sample. Subsequently, 100 μL of the erythrocyte suspension was added to the mixture. The test solution was initially incubated at 37 °C for 60 min and then

https://doi.org/10.1021/acsomega.4c07716
ACS Omega 2025, 10, 3500−3510

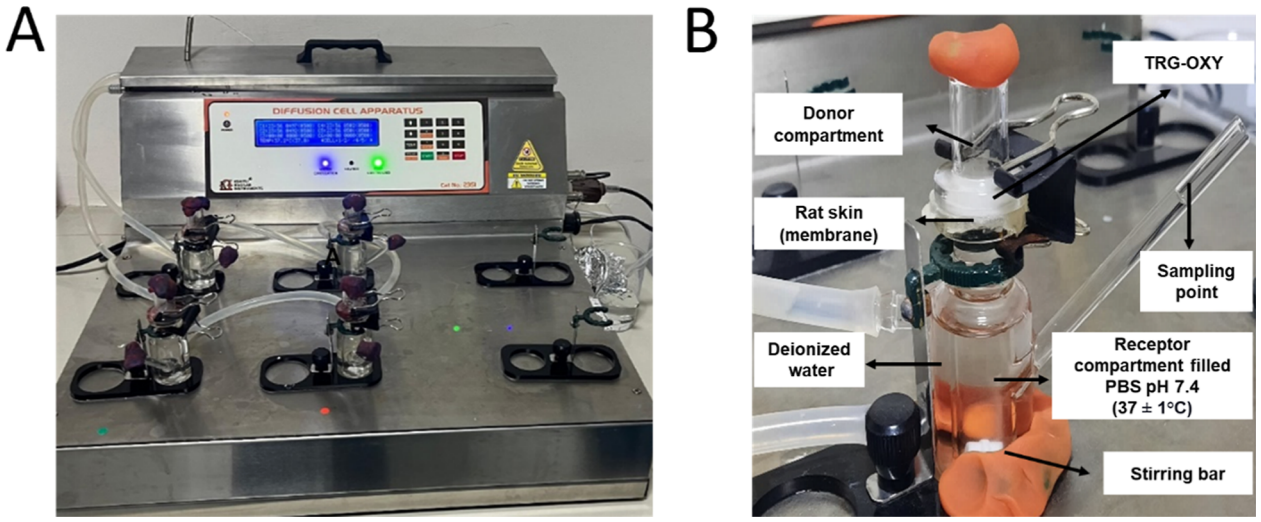

Figure 1. Illustration of the ex vivo permeation test using a diffusion cell apparatus set (A) and a Franz cell (B).

centrifuged at 3000 rpm for 10 min. The absorbance of the resulting supernatant was measured using a UV−vis spectrophotometer (Dynamica, HALO XB-10) to determine hemolysis activity based on the amount of free hemoglobin detected at hemoglobin's maximum wavelength of 540 nm.[38,39] The percentage (%) of HR was calculated as follows (4)

$$\text{hemolysis ratio percentage (\%)} = \frac{OD_{testsample} - OD_{negativecontrol}}{OD_{positivecontrol} - OD_{negativecontrol}} \times 100 \quad (4)$$

2.8. In Vitro Drug Release. In a vial, 5 g of TRG was placed along with 2.5 mL of PBS at pH 7.4 as the medium. Samples of 1 mL each were collected at intervals of 0.25, 0.5, 1, 2, 3, 4, 5, 6, 7, 8, and 24 h. The test temperature was carefully maintained at 37 ± 1 °C. Following each sampling, 1 mL of fresh medium was added to maintain sink conditions.[29] Sample absorbance was determined using a UV−vis spectrophotometer (Dynamica, HALI XB-10, UK) at the maximum wavelength of OXY, 285 nm. OXY concentration was estimated using the calibration curve equation from standard solutions in PBS at pH 7.4 (2.5−80 μg/mL).

2.9. Ex Vivo Permeation Test without PSMN. The permeation test of TRG-OXY was conducted to determine the permeation profile without PSMN. This test used a diffusion cell apparatus with rat skin as the membrane. A solution of PBS at pH 7.4 was added to the receptor compartment, and a magnetic stir bar was placed in a Franz cell. The membrane was placed between the donor and receptor compartments. The temperature of the apparatus was carefully controlled at 37 ± 1 °C while maintaining a stirring speed of 500 rpm (see Figure 1). One gram portion of gel was placed in the donor compartment. Samples of 1 mL each were collected at specified intervals: 0.25, 0.5, 1, 2, 3, 4, 5, 6, 7, 8, and 24 h.[29] After each sampling, 1 mL of fresh PBS at pH 7.4 was added to the receptor compartment to ensure that sink conditions were maintained. Sample absorbance was determined using a UV−vis spectrophotometer (Dynamica, HALI XB-10, UK) at the maximum wavelength of OXY, 285 nm.

2.10. Ex Vivo Permeation Test with PSMN. The ex vivo permeation study was conducted using Franz cells and rat skin to investigate the permeation of OXY from the donor to the receptor compartment (see Figure 1). The receptor compartment was filled with 13 mL of medium (PBS at pH 7.4) and stirred gently at 500 rpm while maintaining a constant temperature of 37 ± 1 °C. PSMN was initially applied to the membrane as a pretreatment to create micropores. After removal of the PSMN, each TRG formulation containing 10 mg of OXY was placed into the donor compartment.[18,29] After each sampling interval (0.25, 0.5, 1, 2, 3, 4, 5, 6, 7, 8, and 24 h), the receptor compartment was replenished with fresh medium to maintain sink conditions. All collected samples were analyzed using a UV−vis spectrophotometer at 285 nm, the maximum wavelength of OXY.

2.11. Data Analysis. The data was processed using Microsoft Excel and shown as mean ± standard deviation (SD). The graphs illustrating the test results were produced by using GraphPad Prism. IBM SPSS Statistics 27 was used for the statistical analysis. The obtained results were assessed for a normality distribution. Subsequently, the results were analyzed using parametric and nonparametric tests based on the normality assessment. One-way ANOVA and Kruskal−Wallis tests were employed to compare the data.

3. RESULTS AND DISCUSSION

3.1. Molecular Docking. Molecular docking is a crucial aspect of drug development, aiding in analyzing the molecular conformation and orientation at binding sites. In this study, molecular docking was utilized to evaluate the binding affinity between OXY (ligand) and Pluronic F127 (receptor), as well as to compare it with other polymers commonly used in TRG formulations, such as PEG.[20,40] Binding affinity represents the strength of the interaction between molecules, with increasingly negative values indicating better binding free energy.[41] The obtained binding affinity energies are presented in Table 3. Based on these results, OXY exhibits good binding affinity to Pluronic F127 (−2.5) compared to that of PEG (−1.6).

The analysis of the hydrogen bonds formed can be seen in Figure 2A,B. The docking results indicate the formation of two hydrogen bonds (Figure 2A) between OXY and PL-127. One hydrogen bond is formed between the amino group (NH) on the pyrimidine ring of OXY and the oxygen atom (O) in the PEO block, with an atomic distance of 2.3 Å (angstroms). Similarly, two hydrogen bonds are formed between OXY and

https://doi.org/10.1021/acsomega.4c07716
ACS Omega 2025, 10, 3500−3510

Table 3. Molecular Docking Simulation Results

polymer-drug	binding energy (kcal/mol)	total number of hydrogen bonds	distance between H atoms (Å)
pluronic F127—OXY	−2.5	1	2.3
polyethylene glycol—OXY	−1.6	2	2.2−2.43

PEG (Figure 2B), with binding sites similar to those between OXY and Pluronic, having atomic distances of 2.2 Å and 2.43 Å. Despite the presence of hydrogen bonds, the binding affinity energy of OXY-PEG is lower (−1.6) compared to that of OXY-Pluronic (−2.3). Therefore, Pluronic was chosen as the TRG-forming agent in this study.

3.2. Effect of Pluronic on Gelation Temperature and Drug Content. Gelation temperature is a crucial parameter in the evaluation of TRG formulations. It indicates the process where the formulation transitions from a solution to a gel system upon surpassing the critical micelle concentration and the critical transition temperature.[42] The optimal gelation temperature for the TRG-OXY formulation should closely approximate the average body temperature (37 °C).[43,44] The findings are depicted in Figure 3A,B, illustrating the appearance of each preparation at room temperature (25 °C) and body temperature (37 °C). The gelation temperatures for formulations G1−G4 were 24.0 ± 1 °C, 25 ± 2.08 °C, 37.3 ± 1 °C, and 41.7 ± 1 °C, respectively. Statistical analysis of the gelation temperature revealed significant differences ($p < 0.05$) between G3 and G4 compared to all other formulations, while G1 and G2 showed no significant difference ($p > 0.05$).

Figure 4A shows the correlation between the concentration of PL-68 and the corresponding increase in gelation temperature. The increased temperature is affected by the varying ratios of PEO and PPO chains in Pluronic. PEO (hydrophilic) increases the gelation temperature, whereas PPO (hydrophobic) decreases it. PL-68 has a higher PEO to PPO ratio compared to PL-127. Therefore, increasing the concentration of PL-68 in the formulation can raise the gelation temperature.[45,46] Among all of the formulations, G3 meets the gelation temperature requirement corresponding to the physiological body temperature.

The drug content measurement results indicate that the OXY concentrations in the TRG formulations G1−G4 were 99.6 ± 0.1%, 99.5 ± 0.1%, 99.6 ± 0.2%, and 99.6 ± 0.2%, respectively. These values comply with the drug content requirement of 85−115%, demonstrating that the presence of Pluronic in the gel formulations did not affect the drug content ($p > 0.05$).[47]

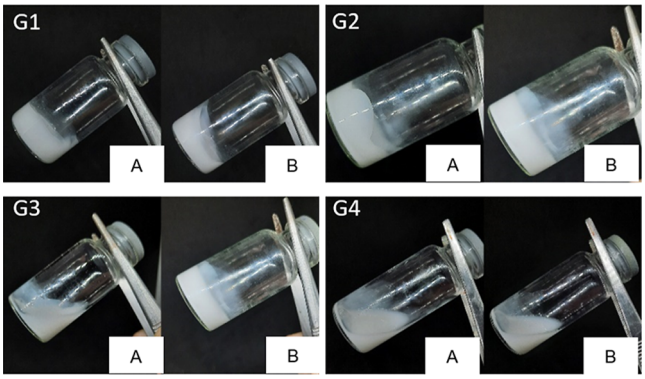

Figure 3. Representative of TRG-OXY at room temperature (A) and body temperature (B).

3.3. pH Determination. The pH values for the thermosensitive OXY gel preparations are displayed in Figure 4B, with results showing pH levels of 7.0 ± 0.14, 5.13 ± 0.73, 4.9 ± 0.45, and 5.28 ± 0.62 for formulations G1−G4, respectively. Statistical analysis indicates that the effect of PL-127 and PL-68 on the gel pH values is insignificant ($p > 0.05$). G2, G3, and G4 fell within the physiological skin pH range of 4.1−5.8.[48] Although G1 does not fall within this range, its pH is neutral and safe for the skin.[49,50] The pH levels of all of the gel formulations were deemed safe for skin application.

3.4. Spreadability Test. The spreadability value is an essential indicator of how evenly the gel is distributed on the skin surface.[50,51] This parameter is also crucial for ensuring the uniform distribution of the drug dose when the gel is applied to the skin.[29,52] The spreadability test was conducted at 37 °C. Figure 4C shows the results of the spreadability test for each formula, ranging from 23.61 mm to 136.15 mm. Based on the statistical test, G1 significantly differed from G4 ($p < 0.05$). Meanwhile, the gels G1−G3 did not exhibit significant differences ($p > 0.05$).

The increase in the spreadability of the gel indicates the influence of the increasing concentration of PL-68 on the preparation. This is due to the longer PEO chains, which affect the gel structure, altering the gel's consistency and spreadability. The G4 formula showed a high spreadability value of 136.15 ± 9.66 mm because it was still in solution form and had not reached the gelation temperature. Conversely, the G1−G3 formulas had already formed gels during testing. Decrease in the spreadability value of the gel indicates good consistency, facilitating application on the skin.[53]

3.5. Bioadhesive Strength Test. The bioadhesive strength test of the TRG-OXY formula is an important parameter, as it

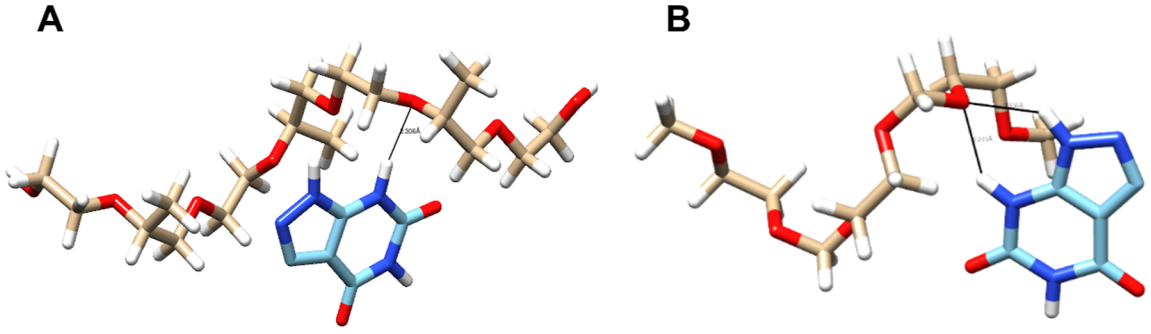

Figure 2. 3D model visualization of the H bonding in OXY-Pluronic F127 (A) and OXY-PEG (B).

https://doi.org/10.1021/acsomega.4c07716
ACS Omega 2025, 10, 3500−3510

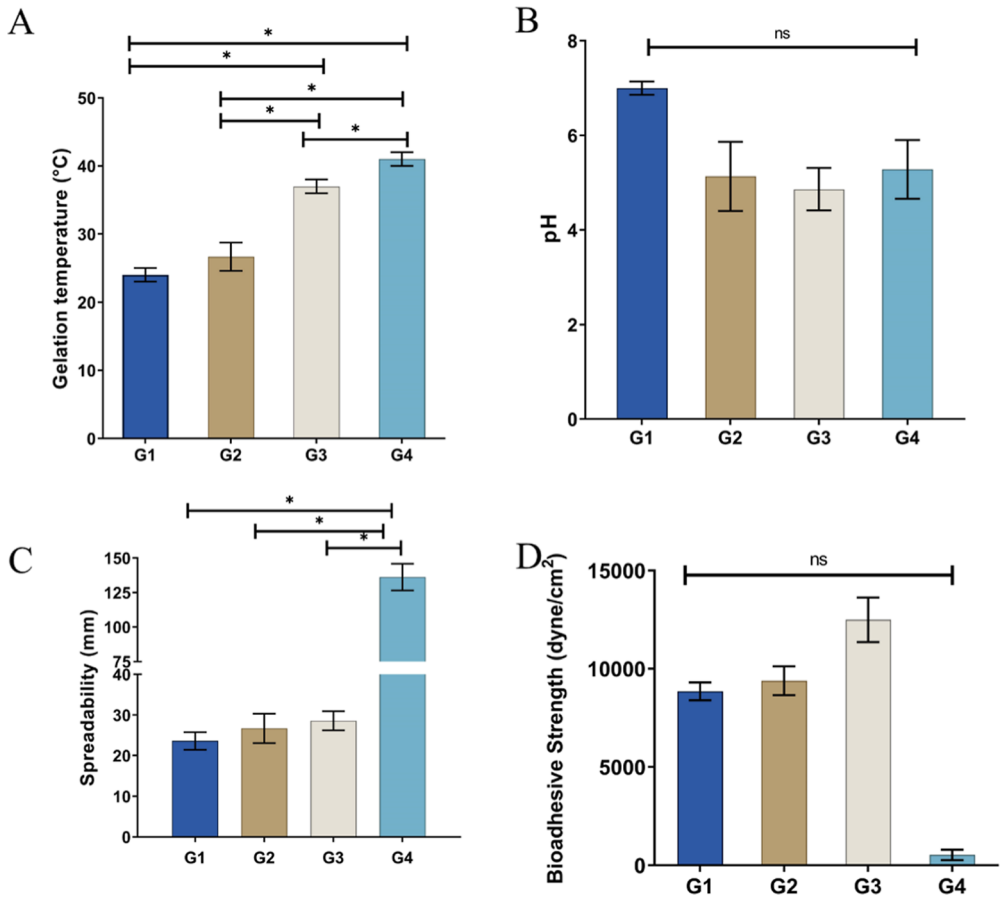

Figure 4. Evaluation of gelation temperature (Tsol−gel) (A), pH of GTH-OXY (B), spreadability of TRG-OXY (C), and bioadhesive strength of TRG-OXY (D) (mean ± SD, $n = 3$).

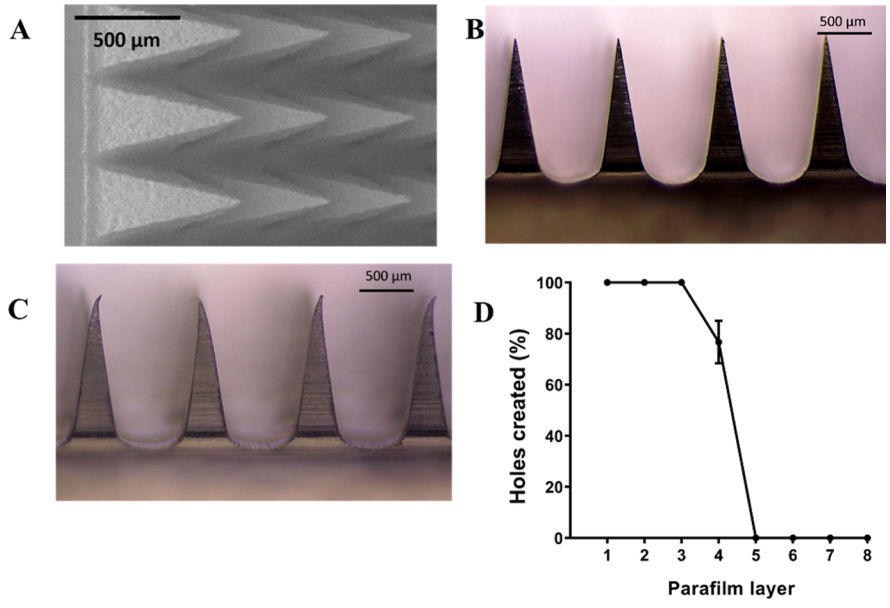

Figure 5. Scanning electron microscopy image of PSMN (A), morphology of PSMN before mechanical testing (B), after mechanical testing (C), and PSMN insertion ability (D) (mean ± SD, $n = 3$).

refers to the gel's ability to adhere to biological surfaces, such as mucous membranes or skin. Bioadhesive strength is crucial for ensuring effective drug delivery through prolonged contact time.[54] Figure 4D shows the bioadhesive strength of each gel formula. In this study, variations in PL-68 concentration did not significantly impact the bioadhesive strength of each formulation ($p > 0.05$). This finding is consistent with previous research that compared the bioadhesive strength of PL-68 and PL-127 at various concentrations. The study concluded that PL-68 does not significantly influence bioadhesive strength, whereas

https://doi.org/10.1021/acsomega.4c07716
ACS Omega 2025, 10, 3500−3510

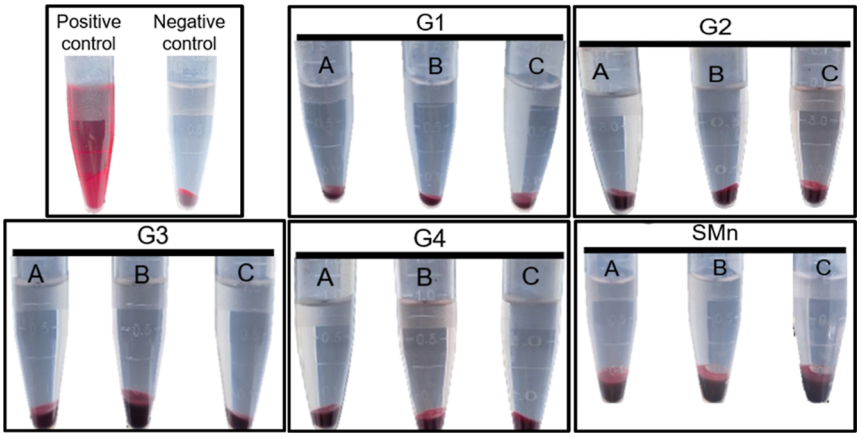

Figure 6. Hemolysis test after incubation with concentrations of 500 μg/mL (A), 50 μg/mL (B), and 5 μg/mL (C).

Table 4. TRG-OXY and PSMN Hemolysis Test Results (Mean ± SD, n = 3)

concentration (μg/mL)	hemolysis ratio (%)				
	G1	G2	G3	G4	PSMN
500	0	3.3 ± 0.1	0	1.34 ± 0.28	3.77 ± 0.2
50	0	2.95 ± 0.1	0.84 ± 0.02	2.58 ± 0.1	4 ± 0.32
5	0	2.58 ± 0.1	1.61 ± 0.01	2.22 ± 0.14	3.88 ± 0.7

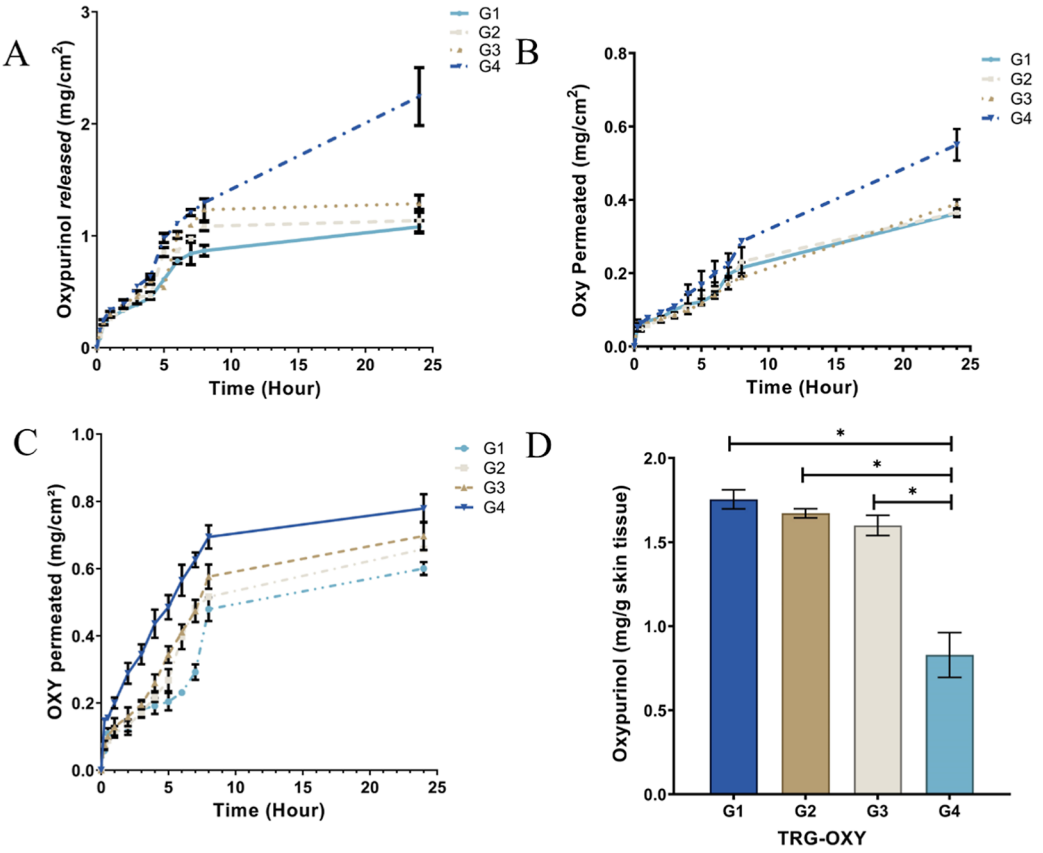

Figure 7. In vitro drug release profile of TRG-OXY (A), permeation profile of TRG-OXY without PSMN (B), permeation profile of TRG-OXY with PSMN (C), and skin retention after 24 h (D) (mean ± SD, n = 3).

increased concentrations of PL-127 affect bioadhesive strength.[19,55]

3.6. Evaluation of the Polymeric Solid Microneedle. Microneedles are a drug delivery system developed to quickly and painlessly penetrate the skin and deliver drugs directly into the bloodstream. Their microscopic size makes this possible, allowing for precise and targeted drug delivery. In this study, PSMNs were used as a pretreatment to enhance the permeation of TRG-OXY into the skin. A combination of PVA and PVP K-30 was used to create the PSMN, adding citric acid as a cross-

https://doi.org/10.1021/acsomega.4c07716
ACS Omega 2025, 10, 3500−3510

linking agent. The hydrogen bonding between PVA (−OH) and PVP (C═O) demonstrates good mechanical strength in the microneedles.[56] The addition of citric acid as a cross-linking agent enhances the strength by forming −OH and esterification reactions.

The characteristics of PSMN evaluated in this study include morphology observation, mechanical strength testing, and insertion testing. Figure 5A shows that PSMN features prismatic and sharp needles, with an average height of 666 μm. The morphology of the microneedles is also depicted in Figure 5B, showing needles with sharp tips and a prismatic shape. With this morphology, the needles are expected to penetrate the SC barrier, thus enhancing drug delivery to the target. Based on the mechanical test, the PSMN experienced a HR of 4.7 ± 2.9%. Figure 5C shows the decreased height of the needle after mechanical strength tests, with less than a 10% reduction, indicating that PSMN has good mechanical properties, allowing them to withstand compression effectively.[37,38]

The following assessment tested the penetration ability of PSMN and was simulated by using parafilm. Figure 5D illustrates that PSMN penetrated up to the fourth layer of parafilm, reaching a depth of 504 μm (with each layer of parafilm being 126 μm thick), corresponding to 75% of the needle height. At this depth, PSMN theoretically can penetrate the epidermal layer, approximately 500 μm.[56,57]

3.7. In Vitro Hemolysis Test. The PSMN and thermosensitive gel−oxypurinol (TRG-OXY) in this study need to be tested for hemolytic activity, as this evaluation is crucial for assessing compounds or materials that may potentially cause damage to erythrocytes. Hemolysis refers to the destruction of red blood cells, releasing hemoglobin and lactate dehydrogenase into the plasma. This can cause auto-oxidation and tissue damage.[58−60] Figure 6 shows the hemolytic activity of each preparation against erythrocytes, indicating clear and transparent results compared to those of positive and negative controls.

The percentage of the HR is shown in Table 4. Formulas G1 and G3 exhibited a ratio of less than 2% in these data, demonstrating the absence of hemolysis activity. On the other hand, G2, G4, and MN showed somewhat hemolysis amounts ranging from 2 to 4%, which is still below the safe threshold of 5%.[61] These results indicate that each tested concentration does not cause hemolysis and is safe for use.[61]

3.8. In Vitro Drug Release. The release study of OXY from the TRG was conducted using a membrane-free dissolution method.[29] The graph in Figure 7A shows the release of OXY from each formula after 24 h. The release profile of OXY in formula G4 showed the highest release at 2.24 ± 0.26 mg ($p < 0.05$) compared to G1 − G3. G1 − G3 released OXY at 1.08 ± 0.05, 1.14 ± 0.10, and 1.29 ± 0.08 mg, respectively. This significant difference is influenced by the gelation of G1 − G3 during testing. When gelation occurs, a matrix forms, which can keep OXY from being released simultaneously. In contrast, G4, which had not yet formed a gel, allowed OXY to release more quickly than the other formulas.[62]

Several studies have stated that PL-127 and PL-68 can control the drug's release gradually or sustained release. Upon reaching the gelation temperature, micelles form a matrix structure, which inhibits the drug molecules from exiting rapidly, causing OXY to be released slowly.[29,62,63] TRG-OXY, with its sustained release profile, can reduce the frequency of repeated drug administration, thereby improving patient comfort and compliance.

3.9. Ex Vivo Permeation and Retention. The first test was without PSMN as pretreatment, while the second involved applying PSMN to the membrane first. This difference was to assess OXY permeation without PSMN and with PSMN. The permeation evaluation was conducted using a Franz diffusion cell apparatus with a diffusion area of 2.08 cm^2 for the test without PSMN and 1.89 cm^2 for the test with PSMN. Figure 7B shows the total permeated OXY without PSMN. G1−G3 exhibited permeation of 0.36 ± 0.01, 0.37 ± 0.01, and 0.39 ± 0.01 mg/cm^2, respectively, with no significant differences ($p > 0.05$). In contrast, G4 had a permeation of 0.55 ± 0.04 mg/cm^2, significantly different from G1 − G3 ($p < 0.05$).

The total permeated OXY after 24 h with PSMN application is shown in Figure 7C. All gels showed an increased permeation profile compared to permeation without PSMN. Statistical analysis indicated significant differences in each formula with and without PSMN ($p < 0.05$). G2 and G3 exhibited the highest increase after MN application, approximately 79−81% of the total OXY permeation without PSMN. This is due to the pores of 504 μm depth based on the insertion test after PSMN was applied to the skin, facilitating OXY penetration through the SC.[28,64] G4 showed high permeation, influenced by the gel system not forming yet during testing as it had not reached the gelation temperature, allowing OXY to release more easily into the skin.[65] Comparing the three formulas that had formed a gel during testing, G3 showed the highest permeation, with a total permeation of 0.70 ± 0.04 mg/cm^2 than G1 and G2 ($p < 0.05$). Based on these permeation test results, G3 is the optimal formulation.

The retention test is the evaluation, followed by the ex vivo gel permeation test. The retention test results can be seen in Figure 7D, where G1−G4 show OXY retention amounts of 1.76 ± 0.06, 1.67 ± 0.03, 1.6 ± 0.06, and 0.83 ± 0.13, respectively. G1−G3 demonstrated high OXY retention in the skin, indicating that Pluronic had no significant impact on retention differences among the formulations ($p > 0.05$). Gels were formed by these three formulations during testing. This indicates that the gel can enhance drug localization in the skin, thereby increasing its concentration within the skin and enhancing the potential of OXY to enter the body.[66]

The studies consistently demonstrate that combining TRG-OXY with PSMN enhances drug permeation, ensures sustained release, and improves the localization of the OXY in skin tissues, potentially facilitating systemic absorption. Among the formulations tested, G3 was identified as optimal due to its gel characteristics, achieving a gelation temperature of 37 °C, which is critical for transdermal application. The pH of G3 is also compatible with skin physiology, and it exhibited excellent spreadability and bioadhesive strength. These properties were enhanced by variations in Pluronic F68 concentration with higher concentrations leading to increased gelation temperatures. Furthermore, hemolysis testing confirmed G3's non-hemolytic nature. The ex vivo permeation tests showed that G3 had the highest permeation rate, increasing significantly from 0.39 ± 0.01 mg/cm^2 (without PSMN) to 0.70 ± 0.04 mg/cm^2 (with PSMN) ($p < 0.05$). These findings suggest that transdermal delivery of OXY via this system is a promising therapeutic approach for gout, particularly for patients requiring long-term treatment. The system's ability to sustain drug release and prolong OXY's half-life could reduce dosing frequency. Overall, the formulation was found to be safe, well-tolerated, and represents an important advancement toward developing a

https://doi.org/10.1021/acsomega.4c07716
ACS Omega 2025, 10, 3500−3510

transdermal drug delivery system for long-term gout management.

4. CONCLUSIONS

In this study, TRG-OXY with PSMN was developed to enhance the delivery of OXY into the skin. The formulation between OXY and Pluronic showed stable bonding through molecular docking analysis. Based on the evaluation of characteristics, drug release studies, and ex vivo permeability tests, it was concluded that the G3 formulation was the most optimal compared with other formulations. The combination of 19% PL-127 and 7.7% PL-68 resulted in a gel that meets the characteristics of a TRG. The drug release profile showing sustained release suggests that OXY can be used with less frequent dosing and potentially improving patient compliance. Furthermore, PSMN demonstrated good mechanical strength and insertion capability, enhancing the delivery of OXY to the target site. The permeation results of OXY from the TRG combined with PSMN as a pretreatment showed a significant increase ($p < 0.05$) of 71−81%. The results of this study suggest a promising new route for delivering OXY using TRG in combination with PSMN, which can be further developed as a more efficient and user-friendly treatment for chronic gout patients.

This study necessitates supplementary data to enhance the delivery of OXY, including in vivo investigations on the efficacy of OXY in reducing blood uric acid levels, comprehensive analysis of its pharmacokinetic and pharmacodynamic profiles, examination of potential drug interactions, toxicity assessments, and long-term stability test to gain a deeper understanding of its potential for clinical use.

AUTHOR INFORMATION

Corresponding Author

Andi Dian Permana − *Department of Pharmaceutical Science and Technology, Faculty of Pharmacy, Hasanuddin University, Makassar 90245, Indonesia;* orcid.org/0000-0003-2168-1688; Email: andi.dian.permana@farmasi.unhas.ac.id

Authors

Siti Nur Fatimah S. Mohamad − *Department of Pharmacy, Faculty of Pharmacy, Hasanuddin University, Makassar 90245, Indonesia*

Stephanie Stephanie − *Postgraduate Program in Pharmacy, Faculty of Pharmacy, Hasanuddin University, Makassar 90245, Indonesia*

Zulfiayu Sapiun − *Departement of Pharmcy, Health Polytechnic of Gorontalo, Kota Gorontalo 405032, Indonesia*

Frederika Tangdilintin − *Postgraduate Program in Pharmacy, Faculty of Pharmacy, Hasanuddin University, Makassar 90245, Indonesia*

Sulistiawati Sulistiawati − *Postgraduate Program in Pharmacy, Faculty of Pharmacy, Hasanuddin University, Makassar 90245, Indonesia*

Achmad Himawan − *Department of Pharmaceutical Science and Technology, Faculty of Pharmacy, Hasanuddin University, Makassar 90245, Indonesia*

Yusnita Rifai − *Department of Pharmaceutical Science and Technology, Faculty of Pharmacy, Hasanuddin University, Makassar 90245, Indonesia*

Habibie Habibie − *Department of Pharmacy, Faculty of Pharmacy, Hasanuddin University, Makassar 90245, Indonesia*

Aliyah Aliyah − *Department of Pharmaceutical Science and Technology, Faculty of Pharmacy, Hasanuddin University, Makassar 90245, Indonesia*

Muhammad Aswad − *Department of Pharmaceutical Science and Technology, Faculty of Pharmacy, Hasanuddin University, Makassar 90245, Indonesia*

Complete contact information is available at: https://pubs.acs.org/10.1021/acsomega.4c07716

Author Contributions

Siti Nur Fatimah S. Mohamad: conceptualization, methodology, visualization, investigation, formal analysis, software data, data curation, writing—original draft, writing—review and editing. **Stephanie Stephanie:** methodology, formal analysis, investigation, writing—review and editing. **Zulfiayu Sapiun:** investigation, methodology, writing—original draft and editing. **Frederika Tangdilintin:** methodology, resources, editing. **Sulistiawati Sulistiawati:** methodology, resources, writing—original draft, editing. **Achmad Himawan:** data curation, analysis, supervision. **Yusnita Rifai:** data curation, investigation, supervision, validation. **Habibie Habibie:** data curation, investigation, supervision, validation. **Aliyah Aliyah:** data curation, investigation, supervision, validation. **Muhammad Aswad:** conceptualization, supervision, writing—review and editing. **Andi Dian Permana:** conceptualization, project administration, resources, supervision, writing—review and editing.

Notes

The authors declare no competing financial interest.

ACKNOWLEDGMENTS

We want to express our deepest gratitude to everyone who contributed to completing this research. Thanks to the Faculty of Pharmacy Hasanuddin University, Indonesia, for invaluable guidance and support throughout the study. We also would like to appreciate the support given by Prof. Latifah Rahman from the Faculty of Pharmacy, Hasanuddin University, Indonesia, for facilitating our research endeavors at the Pharmaceutical Laboratory.

REFERENCES

(1) Ragab, G.; Elshahaly, M.; Bardin, T. Gout: An old disease in new perspective − A review. *J. Adv. Res.* **2017**, *8* (5), 495−511.

(2) Benn, C. L.; Dua, P.; Gurrell, R.; Loudon, P.; Pike, A.; Storer, R. I.; Vangjeli, C. Physiology of hyperuricemia and urate-lowering treatments. *Front. Med.* **2018**, *5*, 160.

(3) Singh, J. A.; Gaffo, A. Gout epidemiology and comorbidities. *Semin. Arthritis Rheum.* **2020**, *50*, S11−S16.

(4) Han, T.; Chen, W.; Qiu, X.; Wang, W. Epidemiology of gout−Global burden of disease research from 1990 to 2019 and future trend predictions. *Ther. Adv. Endocrinol. Metab.* **2024**, *15*, 20420188241227295.

(5) FitzGerald, J. D.; Dalbeth, N.; Mikuls, T.; Brignardello-Petersen, R.; Guyatt, G.; Abeles, A. M.; Gelber, A. C.; Harrold, L. R.; Khanna, D.; King, C.; et al. 2020 American College of Rheumatology Guideline for the Management of Gout. *Arthritis Rheumatol.* **2020**, *72* (6), 879−895.

(6) Hughes, R. W.; Seth, B.; de Gray, L. E. Drugs used to treat joint and muscle disease. *Arthritis Rheumatol.* **2023**, *24*, 806−812.

(7) Stamp, L. K.; Merriman, T. R.; Barclay, M. L.; Singh, J. A.; Roberts, R. L.; Wright, D. F.; Dalbeth, N. Impaired response or insufficient dosage?—Examining the potential causes of "inadequate response" to allopurinol in the treatment of gout. *Semin. Arthritis Rheum.* **2014**, *44*, 170−174.

(8) Day, R. O.; Graham, G. G.; Hicks, M.; McLachlan, A. J.; Stocker, S. L.; Williams, K. M. Clinical pharmacokinetics and pharmacodynamics of allopurinol and oxypurinol. *Clin. Pharmacokinet.* **2007**, *46*, 623−644.
(9) Tayama, Y.; Sugihara, K.; Sanoh, S.; Miyake, K.; Kitamura, S.; Ohta, S. Xanthine oxidase and aldehyde oxidase contribute to allopurinol metabolism in rats. *J. Pharm. Health Care Sci.* **2022**, *8* (1), 31.
(10) Kim, J.; De Jesus, O. *Medication routes of administration*; StatPearls Publishing, 2021.
(11) Herman, T. F.; Santos, C. *First-Pass Effect*; StatPearls Publishing, 2023.
(12) Carr, P. J.; O'Connor, L.; Gethin, G.; Ivory, J. D.; O'Hara, P.; O'Toole, O.; Healy, P. In the preparation and administration of intravenous medicines, what are the best practice standards that healthcare professionals need to follow to ensure patient safety? Protocol for a systematic review. *HRB Open Res* **2020**, *3*, 19.
(13) Zhang, W.; Zhang, W.; Li, C.; Zhang, J.; Qin, L.; Lai, Y. Recent advances of microneedles and their application in disease treatment. *Int. J. Mol. Sci.* **2022**, *23* (5), 2401.
(14) Khanna, P. P.; Perez-Ruiz, F.; Maranian, P.; Khanna, D. Long-term therapy for chronic gout results in clinically important improvements in the health-related quality of life: short form-36 is responsive to change in chronic gout. *Rheumatology* **2011**, *50* (4), 740−745.
(15) Xu, Y.; Zhao, M.; Cao, J.; Fang, T.; Zhang, J.; Zhen, Y.; Wu, F.; Yu, X.; Liu, Y.; Li, J.; et al. Applications and recent advances in transdermal drug delivery systems for the treatment of rheumatoid arthritis. *Acta Pharm. Sin. B* **2023**, *13*, 4417−4441.
(16) Mohammad, C. M.; Shahidah, C. A.; Fatimah, S. W. M. W.; Salman, A.; Zhafri, M. R. M.; Rasimah, I. Delayed hypersensitivity reaction to allopurinol: A case report. *Malays Fam Physician.* **2023**, *18*, 11.
(17) Yu, J.; Qiu, H.; Yin, S.; Wang, H.; Li, Y. Polymeric drug delivery system based on pluronics for cancer treatment. *Molecules* **2021**, *26* (12), 3610.
(18) Enggi, C. K.; Isa, H. T.; Sulistiawati, S.; Ardika, K. A. R.; Wijaya, S.; Asri, R. M.; Mardikasari, S. A.; Donnelly, R. F.; Permana, A. D. Development of thermosensitive and mucoadhesive gels of cabotegravir for enhanced permeation and retention profiles in vaginal tissue: A proof of concept study. *Int. J. Pharm.* **2021**, *609*, 121182.
(19) Permana, A. D.; Utami, R. N.; Layadi, P.; Himawan, A.; Juniarti, N.; Anjani, Q. K.; Utomo, E.; Mardikasari, S. A.; Arjuna, A.; Donnelly, R. F. Thermosensitive and mucoadhesive in situ ocular gel for effective local delivery and antifungal activity of itraconazole nanocrystal in the treatment of fungal keratitis. *Int. J. Pharm.* **2021**, *602*, 120623.
(20) Fan, R.; Cheng, Y.; Wang, R.; Zhang, T.; Zhang, H.; Li, J.; Song, S.; Zheng, A. Thermosensitive hydrogels and advances in their application in disease therapy. *Polymers* **2022**, *14* (12), 2379.
(21) Murphrey, M. B.; Miao, J. H.; Zito, P. M. *Histology, stratum corneum*; StatPearls, 2018.
(22) Aldawood, F. K.; Andar, A.; Desai, S. A comprehensive review of microneedles: Types, materials, processes, characterizations and applications. *Polymers* **2021**, *13* (16), 2815.
(23) Anbazhagan, G.; Suseela, S. B.; Sankararajan, R. Design, analysis and fabrication of solid polymer microneedle patch using CO2 laser and polymer molding. *Drug Delivery Transl. Res.* **2023**, *13* (6), 1813−1827.
(24) Yu, Y.; Cheng, Y.; Tong, J.; Zhang, L.; Wei, Y.; Tian, M. Recent advances in thermo-sensitive hydrogels for drug delivery. *J. Mater. Chem. B* **2021**, *9* (13), 2979−2992.
(25) Zhang, R.; Miao, Q.; Deng, D.; Wu, J.; Miao, Y.; Li, Y. Research progress of advanced microneedle drug delivery system and its application in biomedicine. *Colloids Surf., B* **2023**, *226*, 113302.
(26) Batra, P.; Dawar, A.; Miglani, S. Microneedles and nanopatches-based delivery devices in dentistry. *Discoveries* **2020**, *8* (3), No. e116.
(27) Mdanda, S.; Ubanako, P.; Kondiah, P. P.; Kumar, P.; Choonara, Y. E. Recent advances in microneedle platforms for transdermal drug delivery technologies. *Polymers* **2021**, *13* (15), 2405.
(28) Enggi, C. K.; Satria, M. T.; Nirmayanti, N.; Usman, J. T.; Nur, J. F.; Asri, R. M.; Djide, N. J. N.; Permana, A. D. Improved transdermal delivery of valsartan using combinatorial approach of polymeric transdermal hydrogels and solid microneedles: an ex vivo proof of concept investigation. *J. Biomater. Sci., Polym. Ed.* **2023**, *34* (3), 334−350.
(29) Nirmayanti, N.; Alhidayah, A.; Usman, J. T.; Nur, J. F.; Amir, M. N.; Permana, A. D. Combinatorial approach of thermosensitive hydrogels and solid microneedles to improve transdermal delivery of valsartan: an in vivo proof of concept study. *AAPS PharmSciTech* **2022**, *24* (1), 5.
(30) Agu, P.; Afiukwa, C.; Orji, O.; Ezeh, E.; Ofoke, I.; Ogbu, C.; Ugwuja, E.; Aja, P. Molecular docking as a tool for the discovery of molecular targets of nutraceuticals in diseases management. *Sci. Rep.* **2023**, *13* (1), 13398.
(31) Plugariu, I.-A.; Gradinaru, L. M.; Avadanei, M.; Rosca, I.; Nita, L. E.; Maxim, C.; Bercea, M. Thermosensitive Polyurethane-Based Hydrogels as Potential Vehicles for Meloxicam Delivery. *Pharmaceuticals* **2023**, *16* (11), 1510.
(32) Enggi, C. K.; Sulistiawati, S.; Himawan, A.; Raihan, M.; Iskandar, I. W.; Saputra, R. R.; Rahman, L.; Yulianty, R.; Manggau, M. A.; Donelly, R. F.; et al. Application of Biomaterials in the Development of Hydrogel-Forming Microneedles Integrated with a Cyclodextrin Drug Reservoir for Improved Pharmacokinetic Profiles of Telmisartan. *ACS Biomater. Sci. Eng.* **2024**, *10*, 1554−1576.
(33) Sulistiawati, S.; Enggi, C. K.; Iskandar, I. W.; Saputra, R. R.; Sartini, S.; Rifai, Y.; Rahman, L.; Aswad, M.; Permana, A. D. Bioavailability enhancement of sildenafil citrate via hydrogel-forming microneedle strategy in combination with cyclodextrin complexation. *Int. J. Pharm.* **2024**, *655*, 124053.
(34) Sulistiawati, D.; Kadek, S.; Azhar, M.; Rahman, L.; Pakki, E.; Himawan, A.; Permana, A. D. Enhanced skin localization of metronidazole using solid lipid microparticles incorporated into polymeric hydrogels for potential improved of rosacea treatment: An *ex vivo* proof of concept investigation. *Int. J. Pharm.* **2022**, *628*, 122327.
(35) Anjani, Q. K.; Permana, A. D.; Cárcamo-Martínez, A. ·.; Domínguez-Robles, J.; Tekko, I. A.; Larrañeta, E.; Vora, L. K.; Ramadon, D.; Donnelly, R. F. Versatility of hydrogel-forming microneedles in in vitro transdermal delivery of tuberculosis drugs. *Eur. J. Pharm. Biopharm.* **2021**, *158*, 294−312.
(36) Rynkowska, E.; Fatyeyeva, K.; Marais, S.; Kujawa, J.; Kujawski, W. Chemically and thermally crosslinked PVA-based membranes: effect on swelling and transport behavior. *Polymers* **2019**, *11* (11), 1799.
(37) Sapiun, Z.; Imran, A. K.; Mohamad, S. N. F. S.; Aisyah, A. N.; Stephanie, S.; Himawan, A.; Manggau, M.; Sartini, S.; Rifai, Y.; Permana, A. D. Hispidulin-rich fraction of Clerodendrum fragrans Wild.(Sesewanua) dissolving microneedle as antithrombosis candidate: A proof of concept study. *Int. J. Pharm.* **2024**, *666*, 124766.
(38) Stephanie, S.; Enggi, C. K.; Sulistiawati, S.; Tangdilintin, F.; Achmad, A. A.; Litaay, M.; Kleuser, B.; Manggau, M. A.; Permana, A. D. Fucoidan-incorporated dissolving microneedles: A novel approach to anticoagulant transdermal delivery. *J. Drug Delivery Sci. Technol.* **2024**, *95*, 105587.
(39) Mir, M.; Permana, A. D.; Tekko, I. A.; McCarthy, H. O.; Ahmed, N.; Rehman, A. u.; Donnelly, R. F. Microneedle liquid injection system assisted delivery of infection responsive nanoparticles: A promising approach for enhanced site-specific delivery of carvacrol against polymicrobial biofilms-infected wounds. *Int. J. Pharm.* **2020**, *587*, 119643.
(40) Chen, Y.; Lee, J.-H.; Meng, M.; Cui, N.; Dai, C.-Y.; Jia, Q.; Lee, E.-S.; Jiang, H.-B. An overview on thermosensitive oral gel based on poloxamer 407. *Materials* **2021**, *14* (16), 4522.
(41) Terefe, E. M.; Ghosh, A. Molecular docking, validation, dynamics simulations, and pharmacokinetic prediction of phytochemicals isolated from Croton dichogamus against the HIV-1 reverse transcriptase. *Bioinf. Biol. Insights* **2022**, *16*, 11779322221125605.
(42) Xue, B.; Qu, Y.; Shi, K.; Zhou, K.; He, X.; Chu, B.; Qian, Z. Advances in the application of injectable thermosensitive hydrogel systems for cancer therapy. *J. Biomed. Nanotechnol.* **2020**, *16* (10), 1427−1453.

https://doi.org/10.1021/acsomega.4c07716
ACS Omega 2025, 10, 3500−3510

(43) Lee, C. M.; Jin, S.-P.; Doh, E. J.; Lee, D. H.; Chung, J. H. Regional variation of human skin surface temperature. *Ann. Dermatol.* **2019**, *31* (3), 349.
(44) Koland, M.; Narayanan Vadakkepushpakath, A.; John, A.; Tharamelveliyil Rajendran, A.; Raghunath, I. Thermosensitive in situ gels for joint disorders: pharmaceutical considerations in intra-articular delivery. *Gels* **2022**, *8* (11), 723.
(45) Sharma, P. K.; Reilly, M. J.; Bhatia, S. K.; Sakhitab, N.; Archambault, J. D.; Bhatia, S. R. Effect of pharmaceuticals on thermoreversible gelation of PEO−PPO−PEO copolymers. *Colloids Surf., B* **2008**, *63* (2), 229−235.
(46) Mfoafo, K.; Kwon, Y.; Omidi, Y.; Omidian, H. Contemporary applications of thermogelling PEO-PPO-PEO triblock copolymers. *J. Drug Delivery Sci. Technol.* **2022**, *70*, 103182.
(47) Thakur, A.; Jain, S.; Pant, A.; Sharma, A.; Kumar, R.; Singla, N.; Suttee, A.; Kumar, S.; Barnwal, R. P.; Katare, O. P.; et al. Cyclodextrin derivative enhances the ophthalmic delivery of poorly soluble Azithromycin. *ACS omega* **2022**, *7* (27), 23050−23060.
(48) Lukić, M.; Pantelić, I.; Savić, S. D. Towards optimal ph of the skin and topical formulations: From the current state of the art to tailored products. *Cosmetics* **2021**, *8* (3), 69.
(49) Anitua, E.; Troya, M.; Pino, A. A novel protein-based autologous topical serum for skin regeneration. *J. Cosmet. Dermatol.* **2020**, *19* (3), 705−713.
(50) Hwang, J.-h.; Lee, S.; Lee, H. G.; Choi, D.; Lim, K.-M. Evaluation of skin irritation of acids commonly used in cleaners in 3D-reconstructed human epidermis model, KeraSkinTM. *Toxics* **2022**, *10* (10), 558.
(51) Dantas, M. G. B.; Reis, S. A. G. B.; Damasceno, C. M. D.; Rolim, L. A.; Rolim-Neto, P. J.; Carvalho, F. O.; Quintans-Junior, L. J.; Almeida, J. R. G. d. S. Development and evaluation of stability of a gel formulation containing the monoterpene borneol. *Sci. World J.* **2016**, *2016*, 1−4.
(52) Marzaman, A. N. F.; Mudjahid, M.; Roska, T. P.; Sam, A.; Permana, A. D. Development of chloramphenicol whey protein-based microparticles incorporated into thermoresponsive in situ hydrogels for improved wound healing treatment. *Int. J. Pharm.* **2022**, *628*, 122323.
(53) Djiobie Tchienou, G. E.; Tsatsop Tsague, R. K.; Mbam Pega, T. F.; Bama, V.; Bamseck, A.; Dongmo Sokeng, S.; Ngassoum, M. B. Multi-response optimization in the formulation of a topical cream from natural ingredients. *Cosmetics* **2018**, *5*, 7.
(54) Alagusundaram, M.; Jain, N. K.; Begum, M. Y.; Parameswari, S. A.; Nelson, V. K.; Bayan, M. F.; Chandrasekaran, B. Development and Characterization of Gel-Based Buccoadhesive Bilayer Formulation of Nifedipine. *Gels* **2023**, *9* (9), 688.
(55) Permana, A. D.; Utomo, E.; Pratama, M. R.; Amir, M. N.; Anjani, Q. K.; Mardikasari, S. A.; Sumarheni, S.; Himawan, A.; Arjuna, A.; Usmanengsi, U.; et al. Bioadhesive-thermosensitive in situ vaginal gel of the gel flake-solid dispersion of itraconazole for enhanced antifungal activity in the treatment of vaginal candidiasis. *ACS Appl. Mater. Interfaces* **2021**, *13* (15), 18128−18141.
(56) Mahfufah, U.; Sultan, N. A. F.; Fitri, A. M. N.; Elim, D.; Mahfud, M. A. S. b.; Wafiah, N.; Friandini, R. A.; Chabib, L.; Permana, A. D. Application of multipolymers system in the development of hydrogel-forming microneedle integrated with polyethylene glycol reservoir for transdermal delivery of albendazole. *Eur. Polym. J.* **2023**, *183*, 111762.
(57) Lotfollahi, Z. The anatomy, physiology and function of all skin layers and the impact of ageing on the skin. *Wound Pract. Res.* **2024**, *32* (1), 6−10.
(58) von Petersdorff-Campen, K.; Schmid Daners, M. Hemolysis testing in vitro: A review of challenges and potential improvements. *ASAIO J.* **2022**, *68* (1), 3−13.
(59) Sæbø, I. P.; Bjørås, M.; Franzyk, H.; Helgesen, E.; Booth, J. A. Optimization of the Hemolysis Assay for the Assessment of Cytotoxicity. *Int. J. Mol. Sci.* **2023**, *24* (3), 2914.
(60) Tu, C.; Yang, S.; Yang, M.; Liu, L.; Tao, J.; Zhang, L.; Huang, X.; Tian, Y.; Li, N.; Lin, L.; et al. Mechanisms of persistent hemolysis-induced middle kidney injury in grass carp (Ctenopharyngodon idella). *Fish Shellfish Immunol.* **2024**, *150*, 109603.
(61) Niza, E.; Nieto-Jiménez, C.; Noblejas-López, M. d. M.; Bravo, I.; Castro-Osma, J. A.; de la Cruz-Martínez, F.; Martínez de Sarasa Buchaca, M.; Posadas, I.; Canales-Vázquez, J.; Lara-Sanchez, A.; et al. Poly (cyclohexene phthalate) nanoparticles for controlled dasatinib delivery in breast cancer therapy. *Nanomaterials* **2019**, *9* (9), 1208.
(62) Seon, S.; Li, Y.; Lee, S.; Jeon, Y. S.; Kang, D. S.; Ryu, D. J. Self-Assembled PLGA-Pluronic F127 Microsphere for Sustained Drug Release for Osteoarthritis. *Pharmaceuticals* **2024**, *17* (4), 471.
(63) Permana, A. D.; Elim, D.; Ananda, P. W. R.; Zaman, H. S.; Muslimin, W.; Tunggeng, M. G. R. Enhanced and sustained transdermal delivery of primaquine from polymeric thermoresponsive hydrogels in combination with Dermarollers. *Colloids Surf., B* **2022**, *219*, 112805.
(64) Tariq, N.; Ashraf, M. W.; Tayyaba, S. A review on solid microneedles for biomedical applications. *J. Pharm. Innovation* **2022**, *17* (4), 1464−1483.
(65) Opatha, S. A. T.; Titapiwatanakun, V.; Boonpisutiinant, K.; Chutoprapat, R. Preparation, characterization and permeation study of topical gel loaded with transfersomes containing asiatic acid. *Molecules* **2022**, *27* (15), 4865.
(66) Fiqri, M.; Athiyyah, U.; Layadi, P.; Athiyyah, U.; Layadi, P.; Angeleve Fadjar, T. G.; Permana, A. D. Enhanced localization of cefazoline sodium in the ocular tissue using thermosensitive-mucoadhesive hydrogels: Formulation development, hemocompatibility and in vivo irritation studies. *J. Drug Delivery Sci. Technol.* **2022**, *76*, 103763.

https://doi.org/10.1021/acsomega.4c07716
ACS Omega 2025, 10, 3500−3510